JOURNAL OF Materials CHEMISTRY

Ordered mesoporous hybrid materials containing cobalt(II) Schiff base complex

Robert J. P. Corriu,[a] Emmanuelle Lancelle-Beltran,[a] Ahmad Mehdi,[a] Catherine Reyé,*[a] Stéphane Brandès[b] and Roger Guilard[b]

[a]*Laboratoire de Chimie Moléculaire et Organisation du Solide, UMR 5637 CNRS, Université de Montpellier II, Sciences et Techniques du Languedoc, Place E. Bataillon, F-34095 Montpellier Cedex 5, France. E-mail: corriu@crit.univ-montp2.fr*
[b]*Laboratoire d'Ingénierie Moléculaire pour la Séparation et les Applications des Gaz, LIMSAG, UMR 5633, Université de Bourgogne, 6, Boulevard Gabriel, 21100 Dijon, France. E-mail: limsag@u-bourgogne.fr*

Received 14th January 2002, Accepted 1st March 2002
First published as an Advance Article on the web 2nd April 2002

Immobilisation of Co-salen and Co-fluomine onto ordered mesoporous silica has been achieved through coordination of the cobalt to pyridine or imidazole groups covalently attached to the silica matrix. Two routes have been investigated to obtain mesoporous hybrid materials containing coordinating ligands: post synthesis grafting of 4-[2-(trimethoxysilyl)ethyl]pyridine **1** and *N*-trimethoxysilylpropylimidazole **2** on hexagonally ordered mesoporous silica *via* SiOH groups or direct synthesis method *i.e.* co-hydrolysis and polycondensation of the same functionalised organotrimethoxysilane with a number of equivalents of TEOS in the presence of *n*-hexadecylamine as structure directing agent. The first method gave rise to hexagonally ordered mesoporous hybrid materials. The second afforded mesoporous hybrid materials with a typically disordered wormhole-like framework structure in which the organic groups are probably regularly distributed. The O_2-binding capacity of Co-fluomine immobilized on these materials *via* the imidazole group was investigated.

Introduction

The use of surfactants as structure-directing agents for the synthesis of mesostructured silica has constituted a major discovery in material science over the past decade.[1–5] These materials have high surface areas, uniform and controlled pore sizes and long-range order; they have attracted the attention of numerous scientists due to their potential applications as catalyst supports in particular.[6–8] In other respects, nanostructured organic–inorganic hybrid materials have also received much attention during the same period because they can provide unique combination of properties that cannot be obtained by other routes.[9,10] This last class of materials has been widely used in conjunction with the advance given by the discovery of ordered mesoporous silica. Thus, post-synthesis grafting of an organotrialkoxysilane $RSi(OR')_3$ *via* SiOH groups of ordered mesoporous silica has often been used to obtain ordered mesoporous hybrid materials.[11–14] More recently, another route to obtain ordered mesoporous hybrid materials was achieved by co-hydrolysis and polycondensation of tetraethoxysilane (TEOS) and organotrialkoxysilane $RSi(OR')_3$ in the presence of a structure directing agent.[15–22]

In a continuation of our study on nanostructured hybrid materials,[10] we were particularly interested to prepare hybrid materials able to strongly chelate metal cations. Indeed, such materials have applications in catalysis, or separation techniques; they can also give rise to interesting physical properties in, for example, optics, magnetism or conductivity. With the aim to obtain such materials, we have reported the synthesis[23] and some properties[24] of cyclam-containing hybrid materials, the 1,4,8,11-tetraazacyclodecane (cyclam) being known for its remarkable binding ability towards transition and heavy metal cations.[25,26] We now describe in this paper the immobilisation of cobalt(II) bis(salicylidene)ethylenediamine (Co-salen) and cobalt(II) bis(3-fluorosalicylidene)ethylenediamine (Co-fluomine) on ordered mesoporous silica. Indeed, some metal Schiff base complexes are highly valuable catalysts for oxidation reactions,[27–29] and Co-salen and Co-fluomine are the most extensively studied among the oxygen-binding cobalt complexes.[30,31]

Heterogenisation of homogeneous catalysts constitutes an expanding research area,[32,33] and among the various possibilities, immobilisation of metal complexes in porous hosts is an attractive way to regulate metal based chemistry. Thus, immobilisation of metal Schiff base complex on mesoporous silica gel,[34] and on MCM-41[35,36] has been reported by using a grafting reaction. Immobilisation of Co-fluomine on mesoporous aluminosilicates[37] has also been carried out.

Our approach for the immobilisation of the Co-salen and Co-fluomine on ordered mesoporous silica implies two steps: the first step was the preparation of ordered mesoporous silica functionalised with an appropriate ligand able to coordinate the Schiff base complexes. This first step was achieved according to two methods. The first one is used in the preparation of ordered mesoporous silica of type **SBA-15**,[5] followed by the post-synthesis grafting of silylated ligands **1** and **2** (Scheme 1). The second method consists of preparing ordered mesoporous hybrid materials in one step by co-hydrolysis and polycondensation of **1** or **2** with *y* equivalents of TEOS in the presence of *n*-hexadecylamine[15–17] as structure directing agent (Scheme 2).

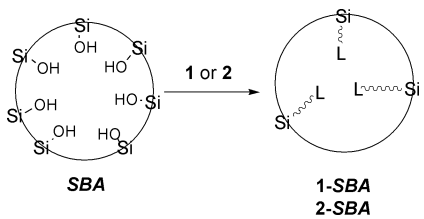

Scheme 1 Post synthesis grafting of ligands **1** or **2** on **SBA**.

This journal is © The Royal Society of Chemistry 2002

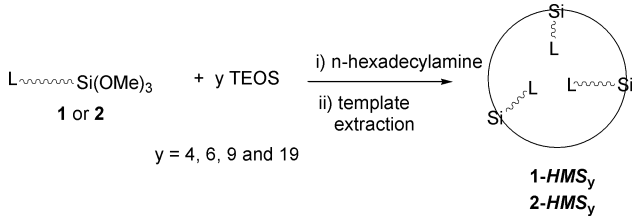

Scheme 2 Preparation of mesoporous hybrid materials by the direct synthesis method.

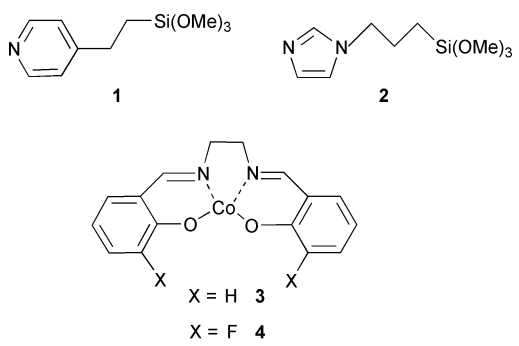

The second step was the binding *via* a co-ordinate bond formation of the Schiff base complexes into the ordered mesoporous functionalised silica prepared by both methods. The preparation and characterization of these materials are presented. Both routes of immobilisation are compared. The O_2-binding capacity of the immobilised Co-fluomine was measured.

Experimental

All reactions were carried out under argon by using a vacuum line. Solvents were dried and distilled just before use. Triblock copolymer ($EO_{20}PO_{70}EO_{20}$) Pluronic P123 was purchased from Aldrich. IR data were obtained on a Perkin-Elmer 1600 FTIR spectrophotometer. The solution NMR spectra were recorded on a BRUKER AC-200 (^{29}Si), BRUKER DPX-200 (^{1}H and ^{13}C). The CP MAS ^{29}Si solid state NMR spectra were recorded on a BRUKER FTAM 300 as well as CP MAS ^{13}C solid state NMR spectra, in the latter case by using the TOSS technique. In both cases, the repetition time was 5 and 10 seconds with contact times of 5 and 2 milliseconds. The EPR spectra were recorded in the solid state on a Bruker ESP 300 spectrometer at X-band (9.6 GHz), from the Centre de Spectrométrie Moléculaire de l'Université de Bourgogne, equipped with a double cavity and a liquid nitrogen cooling accessory. The EPR spectra were referenced to 2,2-diphenyl-1-picrylhydrazyl (DPPH) (g = 2,0036). Sensitive dioxygen compounds were transferred in the EPR tube in a glove box under argon. FAB mass spectra [matrix, *m*-nitrobenzyl alcohol (NBA)] were recorded on a JEOL JMS-D3000 spectrometer. Specific surface areas were determined by the Brunauer–Emmett–Teller (BET) method on Micromeritics ASAP 2010 analyser. Elemental analyses were carried out by the Service Central de Micro-Analyse du CNRS, Lyon.

4-[2-(Trimethoxysilyl)ethyl]pyridine 1

To a mixture of 4-[2-(trichlorosilyl)ethyl]pyridine (18.5 g, 77 mmol) and triethylamine (80 mL) in dry pentane (120 mL) was added dropwise methanol (20 mL, 462 mmol) at 0 °C. The reaction mixture was then stirred at 20 °C for 20 hours. The final white suspension was filtered off and the filtrate concentrated under vacuum to give a crude oil. Distillation of the residue afforded 14.1 g (61.5 mmol, 80%) of **1**. Bp 108 °C (0.3 mbar). ^{1}H NMR (δ, 200 MHz, $CDCl_3$) 0.86–0.95 (m, 2H, CH_2Si), 2.60–2.68 (m, 2H, CH_2), 3.40 (s, 9H, OMe), 7.04–7.07 (m, 2H, Ar), 8.39–8.42 (dd, 2H, Ar). ^{13}C NMR (δ, 50 MHz, $CDCl_3$) 10.4 (CH_2Si), 28.4 (CH_2), 50.8 (OMe), 123.6 (Ar), 150.0 (Ar), 153.4 (Ar). ^{29}Si NMR (δ, 40 MHz, $CDCl_3$) −43.5 (s). MS (FAB+, NBA): m/z = 228 [$(M+H)^+$, 100%], 121 [$Si(OMe)_3^+$, 8%], 106 [$M - (Si(OMe)_3)^+$, 10%]. IR (cm^{-1}, oil): 3060–3020 (ν C_{sp2}–H), 2943–2845 (ν C_{sp3}–H), 1600–1556 (ν C=C), 1088 (ν Si–O). Anal. calcd. For $C_{10}H_{17}NO_3Si$: C, 52.83; H, 7.54; N, 6.16; Si, 12.35. Found: C, 52.65; H, 8.17; N, 6.32; Si, 12.05%.

N-Trimethoxysilylpropylimidazole 2

2 was elaborated in two steps:

In the first step, to a solution of imidazole (9.1 g, 130 mmol) in THF (80 mL) was added slowly a suspension of NaH (4.4 g at 60% wt, 110 mmol) in THF (40 mL) at 0 °C. After stirring for 20 hours at 20 °C, the suspension was filtered off and the precipitate washed with THF (3 × 20 mL). After drying, 9.5 g of sodio-imidazole salt were obtained as a white powder in 95% yield.

In the second step, 13.1 g (45 mmol) of iodopropyltrimethoxysilane were added dropwise to a suspension of sodio-imidazole salt (4.1 g, 45 mmol) in THF (60 mL) at 0 °C. The mixture was stirred at 20 °C for two hours. The solvent was then evaporated under vacuum and the residue was taken up again in CH_2Cl_2 (150 mL). After filtration of the salts, the filtrate was concentrated under vacuum. Distillation of the residue afforded 8.2 g (35.5 mmol, 79%) of **2**. Bp 116–119 °C (0.4 mbar). ^{1}H NMR (δ, 200 MHz, $CDCl_3$) 0.40–0.48 (m, 2H, CH_2Si), 1.67–1.82 (m, 2H, CH_2), 3.40 (s, 9H, OMe), 3.79 (t, $^{3}J_{HH}$ = 7.0 Hz, 2H, CH_2N), 6.79 (s, 1H, Ar), 6.90 (s, 1H, Ar), 7.34 (s, 1H, Ar). ^{13}C NMR (δ, 50 MHz, $CDCl_3$) 6.3 (CH_2Si), 24.9 (CH_2), 49.3 (CH_2N), 50.8 (OMe), 119.0 (Ar), 129.6 (Ar), 137.4 (Ar). ^{29}Si NMR (δ, 40 MHz, $CDCl_3$) −43.5 (s). MS (FAB+, NBA): m/z = 231 [$(M + H)^+$, 100%], 121 [$Si(OMe)_3^+$, 33%]. IR (cm^{-1}, oil): 3106 (ν C_{sp2}–H), 2943–2845 (ν C_{sp3}–H), 1507 (ν C=C), 1463, 1447 (ν C=N), 1082 (ν Si–O). Anal. calcd. for $C_9H_{18}N_2O_3Si$: C, 46.93; H, 7.88; N, 12.16; Si, 12.19. Found: C, 47.12; H, 8.04; N, 12.25; Si, 12.55%.

Preparation of the silica SBA

P123 (4.10 g, 0.068 mmol) was dissolved in 150 mL of an aqueous solution of HCl (pH = 1.5). The resulting clear solution was then added to TEOS (9.35 g, 44.9 mmol). The mixture was vigorously stirred for 3 hours at room temperature until a transparent solution appears. After heating the solution at 60 °C, NaF (76 mg, 1.8 mmol) was then added. (The molar composition of the mixture was: 1 TEOS, 1.5 × 10^{-3} P123, 185 H_2O, 4.7 HCl and 4 × 10^{-2} NaF.) After aging under regular stirring for 3 days at 60 °C, the resulting powder was filtered off and the surfactant was removed by Soxhlet extraction over ethanol for 24 hours. After drying at 120 °C under vacuum, **SBA** (2.80 g) was obtained.

Post-synthesis grafting of SBA

1-SBA was prepared by addition of **1** (220 mg, 1 mmol) to a suspension of **SBA** (700 mg) in toluene (50 mL). The mixture was refluxed and stirred for 24 hours. After filtration, the solid was washed with acetone and diethyl ether, and then dried at 120 °C under vacuum to give 850 mg of **1-SBA**. ^{13}C NMR (δ, 75 MHz, CP-MAS) 16.0 (CH_2Si), 28.4 (CH_2), 58.1 (OMe), 123.6 (Ar), 148.5–155.2 (Ar). NMR ^{29}Si (δ, 60 MHz, CP-MAS) −63.0 and −70.0 (T^2 and T^3), −102.0 (Q^3), −112.0 (Q^4). Anal. found: Si, 38.34; N, 1.42%.

2-SBA was prepared by addition of **2** (156 mg, 6.7 × 10^{-1} mmol) to a suspension of **SBA** (485 mg) in toluene (40 mL). The mixture was refluxed and stirred for 24 hours. After filtration, the solid was washed with acetone and diethyl ether, and then dried at 120 °C under vacuum to give 535 mg of

2-SBA. ^{13}C NMR (δ, 75 MHz, CP-MAS) 7.5 (CH_2Si), 23.5 (CH_2), 47.8 (NCH_2 and OMe), 118.4 (Ar), 126.8–137.4 (Ar). ^{29}Si NMR (δ, 60 MHz, CP-MAS): −57.0 and −68.0 (T^2 and T^3), −102.0 (Q^3), −111.0 (Q^4). Anal. found: Si, 36.00; N, 3.43%.

Preparation of 1-HMS and 2-HMS

Both the solids were prepared according to the same procedure.

1-HMS_9

In a typical preparation, a mixture of **1** (290 mg, 1.28 mmol) and TEOS (2.39 g, 11.52 mmol) was added under stirring to 12.8 ml (34.5 mmol) of a 0.27 M solution of *n*-hexadecylamine in a 55 : 45 EtOH (95%)–H_2O mixture at 35 °C. A white precipitate appears within some minutes. The reaction mixture was kept at 35 °C for 24 h. The solid was then filtered and *n*-hexadecylamine was removed by Soxhlet extraction over ethanol for 24 hours. After drying at 120 °C under vacuum, **1-HMS_9** (860 mg) was obtained. ^{13}C NMR (δ, 75 MHz, CP-MAS) 15.7 (CH_2Si), 28.4 (CH_2), 57.7 (OMe), 124.0 (Ar), 147.4–153.8 (Ar). ^{29}Si NMR (δ, 60 MHz, CP-MAS): −62.0 and −68.0 (T^2 and T^3), −102.0 (Q^3), −112.0 (Q^4). Anal. calcd: C, 12.03; N, 2.00; Si, 40.18. Found: C, 12.62; N, 1.70; Si, 34.20%.

Trimethylsilylation of 2-SBA and 2-HMS with hexamethyldisilazane (HMDS)

All the solids were silylated according to the same procedure.

2-HMS_6-Si

In a typical silylation, **2-HMS_6** (400 mg) was mixed with HMDS (20 mL) and stirred under reflux for 24 hours. The suspension was then filtered off and the solid was washed with ethanol (3 × 20 mL), acetone and diethyl ether. After drying at 120 °C under vacuum, **2-HMS_6-Si** (445 mg) was obtained.

Coordination of Co-salen 3 and Co-fluomine 4

All the solids were coordinated with **3 or 4** according to the same procedure.

2-HMS_6-[4]

In a typical coordination of **4**, a solution of **4** (360 mg, 1 mmol) in dry toluene (90 mL) was added at room temperature to a suspension of **2-HMS_6** (400 mg) in dry toluene. The mixture was stirred under reflux for 24 hours. The suspension was then filtered off and the solid was washed with CH_2Cl_2 (200 mL). After drying under vacuum at 120 °C,**2-HMS_6-[4]** (450 mg) was obtained as a dark orange powder. The solid became black purple in contact with air. Anal. calcd.: Co, 7.73; N, 7.34. Found: Co, 2.60; N, 5.96%.

Results and discussion

Preparation of mesoporous hybrid materials incorporating a coordinating group

Preparation of materials 1-SBA and 2-SBA. We prepared a hexagonally ordered mesoporous silica by hydrolysis and polycondensation of tetraethoxysilane (TEOS) in the presence of the non-ionic surfactant P123 as structure-directing agent under acidic conditions. Our procedure was inspired by the procedure described by Prouzet *et al.* which involved tergitol ($C_{15}H_{31}O(CH_2CH_2O)_{12}H$) as structure-directing agent and gave rise to **MSU** silica.[38] It involves two steps: first the formation of a microemulsion from both the non-ionic surfactant P123 and the TEOS under acidic conditions, then addition of a catalytic amount of fluoride ion to induce the polycondensation. We have named this silica **SBA** as Stucky *et al* have described a hexagonally ordered mesoporous silica prepared in the presence of P123 and called it **SBA-15**.[5] The powder X-ray pattern of the silica **SBA** exhibits an intense diffraction peak corresponding to d_{100} spacing and two weak higher order reflexions, indicating a 2D hexagonal structure (Fig. 1a). The N_2 adsorption–desorption isotherm for **SBA** was of type IV, characteristic of mesoporous materials with a narrow pore size distribution (Fig. 2a). It is worth noting that this procedure gives rise to a silica with a large mean pore diameter (108 Å). Some relevant physical data for **SBA** are reported in Table 1.

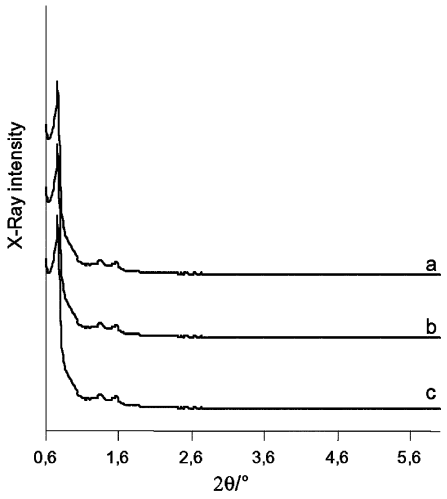

Fig. 1 Powder XRD diffraction patterns for **SBA** (a), **2-SBA** (b) and **2-SBA-[4]** (c).

Grafting[11–14] of organic ligands onto walls of silica **SBA** was achieved by treating the mesoporous silica with a toluene solution of **1** or **2** to afford, respectively, the materials **1-SBA** and **2-SBA**. Some relevant physical data of the functionalised silica are given in Table 1. The XRD analysis exhibited an intense reflexion (100) and two higher order reflexions indicating that the chemical bonding procedure did not diminish the structural ordering of the silica (Fig. 1b). The N_2 adsorption–desorption isotherms for **1-SBA** and **2-SBA** are of type IV, characteristic of mesoporous materials with a narrow pore size distribution. The surface area, total pore volume and pore size decreased significantly after grafting. These observations are consistent with the presence of a significant amount of grafted species attached to the framework walls of the silica. This was confirmed by the determination of the content of organic groups from elemental analysis

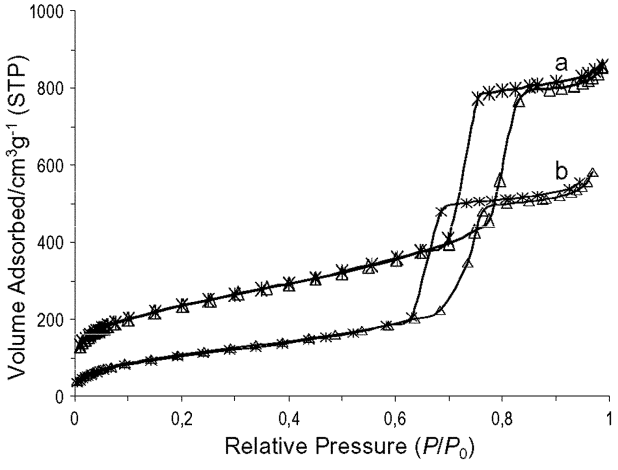

Fig. 2 Nitrogen adsorption–desorption isotherms of **SBA** (a) and **2-SBA-[4]** (b).

Table 1 Physicochemical data of the silica **SBA** and of mesoporous silica after grafting of the coordinating ligand **1** and **2**

Sample	d_{100}/Å	d_{110}/Å	d_{200} /Å	S_{BET}/ $m^2\ g^{-1}$	V_p / $cm^3\ g^{-1}$	d_p/Å[a]	Organic loading mmol g^{-1}[b]
SBA	119	65	55	835	1.32	108	-
1-SBA	116	65	56	533	0.92	95	1.0
2-SBA	113	64	55	475	0.86	95	1.4

[a]Calculated from the adsorption branch of the N_2 isotherm by using the BJH method. [b]Calculated from elemental analysis.

Table 2 Physicochemical data of mesoporous hybrid materials prepared by the direct synthesis method

Entries	Sample	d_{100} /Å	S_{BET} / $m^2\ g^{-1}$)	V_p / $cm^3\ g^{-1}$	D_p /Å[a]	Organic loading[b] mmol g^{-1}
1	**1-HMS$_9$**	43	1142	1.11	29	1.2
2	**1-HMS$_{19}$**	42	1178	0.64	27	0.6
3	**2-HMS$_4$**	50	1012	1.15	26	2.2
4	**2-HMS$_6$**	47	990	0.85	25	1.6
5	**2-HMS$_9$**	49	1021	1.03	26	1.4
6	**2-HMS$_{19}$**	48	985	1.03	26	0.6

[a]Calculated from the adsorption branch of the N_2 isotherm by using the BJH method. [b]Calculated from elemental analysis.

(Table 1). Furthermore, the ^{13}C NMR spectroscopy of materials **1-SBA** and **2-SBA** revealed that the grafted organic moieties are intact, the chemical shifts of ligands are the same as those observed in solution for, respectively, **1** and **2** (see Experimental section).

Direct synthesis method of preparing mesoporous hybrid materials incorporating coordinating ligands. The direct synthesis method of functionalisation of ordered mesoporous silica in the presence of a structure-directing agent constituted a new and very promising route to hybrid materials.[15–22] This method consists of the co-hydrolysis and polycondensation of an organotrialkoxysilane $RSi(OR')_3$ and of *y* equiv. of TEOS in the presence of a surfactant. This method requires that during the hydrolytic polycondensation, the R groups are located inside the micelle to obtain a uniform distribution of R groups within the pores after removal of the surfactant. In order to avoid the protonation of the organic groups, it was necessary to work under neutral conditions. For this reason, we have chosen as surfactant, the *n*-hexadecylamine.[15–17] The co-hydrolysis and polycondensation of **1** or **2** with *y* equivalents of TEOS, in the presence of *n*-hexadecylamine (Scheme 2) afforded respectively the materials **1-HMS$_y$** and **2-HMS$_y$**, *y* indicates the number of equivalents of TEOS. Table 2 summarizes the physical parameters of the materials. The X-ray diffraction patterns of all these materials display only a broad reflexion, typical of disordered wormhole-like pore structures (Fig. 3).[3,4,15–17,21,22] The N_2 adsorption–desorption isotherms are of type IV with little hysteresis revealing the mesoporosity of the materials (Fig. 4a). A very large BET surface area was found, over 985 $m^2\ g^{-1}$ with pore volumes greater than 0.64 $cm^3\ g^{-1}$. Pore size distributions were calculated using the BJH method.[39] The organic loading was calculated from elemental analyses data. It is worth noting that the direct synthesis allows an organic loading superior to that obtained by post synthesis grafting though the pores size of the silica **SBA** was rather large. As an example, from **SBA** it was possible to graft no more than 1.4 mmol g^{-1} of imidazole ligand (material **2-SBA**) while by the direct synthesis 2.2 mmol g^{-1} of imidazole ligand have been incorporated (material **2-HMS$_4$**). Furthermore, the direct synthesis method allows the control of the amount of organic groups incorporated in the structure (Table 2).

Silylation of materials 2-HMS$_y$ and 2-SBA

Before the immobilization of Schiff-base complexes onto the functionalised silica, it seemed to us necessary to deactivate the SiOH groups on the pores surface with trimethylsilyl moieties in order to avoid the possible coordination of SiOH on the metal centres. For this purpose, selected hybrid materials were treated with a large excess of hexamethyldisilazane (HMDS)[40] heated under reflux for 24 h. The materials formed by the treatment are named as above followed by "**Si**" to indicate the capping of SiOH groups with trimethylsilyl moieties. The XRD patterns of materials **2-HMS$_y$-Si** and **2-SBA-Si** showed that their mesoporous structure were retained with the same d_{100} values as those of the corresponding parent material, indicating that the silylation occurred without collapse of the original hexagonal structures (Table 3). If we compare the surface

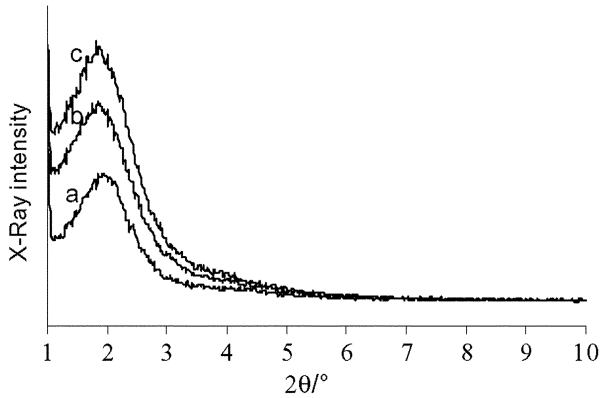

Fig. 3 Powder XRD diffraction patterns for **2-HMS$_6$** (a), **2-HMS$_9$** (b) and **2-HMS$_{19}$** (c).

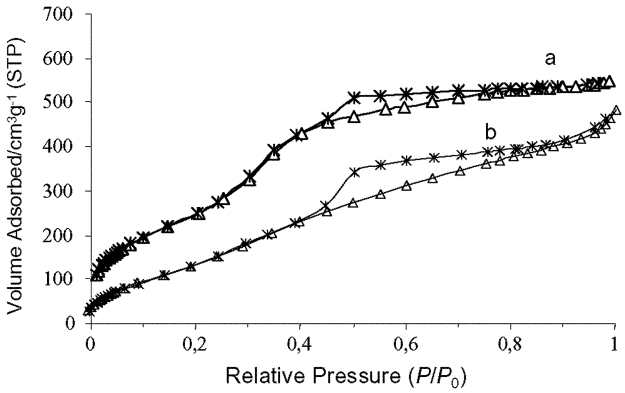

Fig. 4 Nitrogen adsorption–desorption isotherms of **2-HMS$_9$** (a) and **2-HMS$_9$-[4]** (b).

Table 3 Physicochemical properties of mesoporous hybrid materials after silylation of the surface

Sample	S_{BET}/m^2 g^{-1}	V_p /cm^3 g^{-1}	D_p /Å[a]	d_{100} /Å
2-HMS$_4$-Si	817	0.89	23	49
2-HMS$_6$-Si	863	0.61	22	48
2-HMS$_9$-Si	820	0.77	22	49
2-HMS$_{19}$-Si	767	0.65	21	47
2-SBA-Si	300	0.63	93	116

[a]Calculated from the adsorption branch of the N_2 isotherm by using the BJH method.

areas, the pore volumes and the mean pore diameters of materials after capping (Table 3) with the data of the corresponding materials before silylation (Table 2), it appears that, as expected, the surface areas and pore volumes decreased substantially indicating the successful silylation. FTIR measurements showed a notable decrease in the broad and intense band at 3400 cm^{-1} corresponding to bound SiOH groups, this indicates that a large number of SiOH groups have reacted with HMDS but that the silylation was nevertheless incomplete. The ^{13}C and ^{29}Si CP MAS NMR spectroscopies confirm the presence of $Si(CH_3)_3$ groups with the appearance of an intense new peak in both cases, respectively at 0 ppm and 13 ppm.

Thermal analysis was performed on the material **2-SBA-Si**. It revealed no significant loss of H_2O between 20 °C and 200 °C. This result, in agreement with the study of Koyano *et al*[41], confirmed the hydrophobic character of materials after silylation.

Coordination of Co-salen and Co-fluomine onto mesostructured hybrid materials

First, we checked that the immobilization of Co-complexes did not occur in the pure mesoporous silica. Therefore, we treated the silica-**SBA** with a toluene solution of Co-complex (**3** and **4**) heated under reflux for 24 h. After filtration, the solid was washed with CH_2Cl_2 until the filtrate was colourless; elemental analyses of the silica revealed no trace of cobalt.

Immobilisation of the Co-salen **3** and Co-fluomine **4** onto the materials was achieved through coordination of the cobalt ion to the pyridine or imidazole group covalently attached to the pores surface of materials. This method was successfully used for the immobilisation of other metal complexes on organic or inorganic supports.[36,42–44]

The coordination of Co-salen was investigated under different experimental conditions. Typically, a solution of one equiv. of Schiff base complex (calculated for a completely condensed material) was added to a suspension of the functional mesoporous silica. After reaction, the solid was filtrated and copiously washed with CH_2Cl_2 until the filtrate became colourless. The materials were dried at 120 °C under vacuum, then they were characterised. It is worth noting that the powder XRD diffraction patterns of solids after coordination of the Co-salen display the absence of the reflexion characteristic of the crystalline Co-salen (Fig. 5), which proves the complete elimination of the free Co-salen by washing.

After coordination, the materials were named as the parent material with the number **3** for Co-salen. The concentration

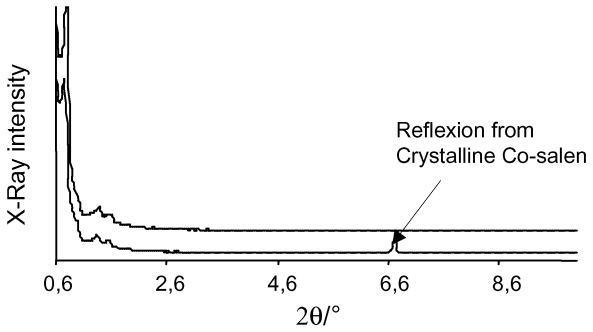

Fig. 5 Powder XRD diffraction patterns for **1-SBA-[3]** before (bottom) and after (top) washing.

of Co and the percentage of complexed sites were inferred from elemental analyses of cobalt and nitrogen. The results are reported in Table 4. It appears that the percentages of coordination were slightly better when the reaction was carried out in toluene heated under reflux for 24 h (compare entries 1 and 2; 4 and 5) than in CH_2Cl_2. Furthermore, the imidazole group appears to be a slightly better coordinating group (compare entries 4 and 6).

Therefore, the coordination of Co-fluomine was achieved by using the corresponding materials with imidazole groups. These materials were treated with a toluene solution of **4** heated under reflux for 24 h. After filtration, the solids were washed with CH_2Cl_2 until the filtrate became colourless. They were named as the parent material followed by the number **4** for Co-fluomine.

The IR spectroscopy of materials **2-HMS$_y$-[4]** and **2-SBA-[4]** indicated qualitatively the presence of Co-fluomine. Indeed, a band at 1636 cm^{-1} appeared and was assigned to the C=N stretching vibration. The intensity of this band is clearly related to the composition of the starting material for the series **HMS$_y$-[4]**. The higher the concentration in imidazole, the stronger the C=N stretching vibration.

The concentration of Co and the percentage of complexed sites were inferred from elemental analyses of cobalt and nitrogen. The results are reported in Table 5.

It appears that the concentration of cobalt decreased for the series of materials **2-HMS$_y$-[4]**, (compare the entries 1, 2, 4 and 6 in Table 5) with the organic loading (Table 2). In contrast, the percentage of complexed sites increased for this same series of samples whereas the organic loading decreased (compare entries 1, 2, 4, and 6 in Table 5 to entries 3, 4, 5, 6 in Table 2). This could be explained by steric constraints within the pores when the organic loading becomes significant, the mean pore diameters is rather small (about 25 Å).

The capping of the SiOH with trimethylsilyl groups in both types of materials produced a notable decrease in the Co-fluomine coordination even from the material **2-SBA** with rather large pores (compare entries 2 and 3, entries 4 and 5, entries 6 and 7 and entries 8 and 9 in Table 5). This is probably also due to steric constraints with the trimethylsilyl groups.

It is of interest to compare the concentration of cobalt within the materials **2-HMS$_9$-[4]** and **2-SBA-[4]** respectively obtained

Table 4 Physicochemical data of mesoporous hybrid materials after coordination of the Co-salen

Entry	Sample	Coord. conditions	[Co] mmol g^{-1}	% of coordination	d_{100} /Å	S_{BET}/m^2 g^{-1}	V_p/cm^3 g^{-1}	D_p /Å
1	**1-HMS$_9$-[3]**	CH_2Cl_2,40 °C, 24 h	0.09	9.2	44	855	0.83	22
2	**1-HMS$_9$-[3]**	Toluene, 110 °C, 24 h	0.13	17.7	[a]	440	0.73	24
3	**1-HMS$_{19}$-[3]**	CH_2Cl_2,40 °C, 24 h	0.04	7.8	43	1110	0.59	26
4	**1-SBA-[3]**	CH_2Cl_2,40 °C, 24 h	0.11	8.4	114	403	0.73	84
5	**1-SBA-[3]**	Toluene, 110 °C, 24 h	0.13	10.1	113	390	0.71	84
6	**2-SBA-[3]**	CH_2Cl_2,40 °C, 24 h	0.13	10.5	113	368	0.70	85

[a]No reflexion.

Table 5 Physicochemical data of mesoporous hybrid materials after coordination of the Co-fluomine

Entry	Sample	[Co][a] mmol g^{-1}	% of coordination	d_{100} /Å	S_{BET} /m^2 g^{-1}	V_p /cm^3 g^{-1}	D_p /Å
1	**2-HMS$_4$-[4]**	0.44	26.2	49	602	0.71	25
2	**2-HMS$_6$-[4]**	0.38	28.1	49	958	0.76	23
3	**2-HMS$_6$-Si-[4]**	0.21	17.5	49	688	0.55	<20
4	**2-HMS$_9$-[4]**	0.34	31.5	51	904	0.88	25
5	**2-HMS$_9$-Si-[4]**	0.15	14.9	49	712	0.69	<20
6	**2-HMS$_{19}$-[4]**	0.26	48.1	48	793	0.76	25
7	**2-HMS$_{19}$-Si-[4]**	0.15	28.9	47	711	0.63	<20
8	**2-SBA-[4]**	0.39	35.1	116	254	0.51	87
9	**2-SBA-Si-[4]**	0.13	11.7	116	271	0.56	87

[a]Complexation in toluene heated under reflux for 24 h.

by the direct synthesis method and by grafting on **SBA** followed in both cases by the coordination of **4**. Both materials contained 1.4 mmol g^{-1} of ligand, but with a mean pore size of 25 Å for **2-HMS$_9$-[4]** and of 95 Å for **2-SBA-[4]**. It appears that the increase in the cobalt concentration going from **2-HMS$_9$-[4]** to **2-SBA-[4]** (entries 4 and 8, Table 5) is not in agreement with the increase in the pore size. This could indicate that the surface coverage of imidazole ligands was not regularly distributed within the pores of the material **2-SBA**, prepared by post synthesis grafting from the silica **SBA**. The irregular distribution of imidazole ligand should involve, as a consequence, steric constraints for the Co-fluomine coordination in spite of the rather large pore size, which should explain the rather weak cobalt concentration within **2-SBA-[4]** in comparison to the mean pore size. Thus, this result showed that the direct synthesis method for preparation of mesoporous hybrid materials in the presence of a surfactant is, no doubt, a more attractive route to obtain a regular distribution of the organic groups inside the channels.[20]

The X-ray powder diffraction patterns of the materials of the type **HMS** showed, after coordination of a Schiff base complex, a broad reflexion as for the parent material (Fig. 6). A particularly weak intensity was observed for the reflexion for the material **2-HMS$_4$-[4]** containing the highest ratio of coordinated Co-fluomine. This was probably due to contrast matching between the inorganic framework and the organic ligand.

The powder XRD patterns of the materials of the type **SBA** displayed, after coordination of a Schiff base complex, the same patterns as before coordination (Fig. 1c), indicating that the structure of the materials survived the coordination reaction.

The N_2 adsorption–desorption isotherms for materials of type **SBA** and **HMS**, after coordination of a Schiff base complex are of type IV, characteristic of mesoporous materials (Fig. 2b and Fig. 4b). The surface area, total pore volume and pore size were found to decrease after coordination (Tables 4 and 5).

O_2 adsorption on immobilised Co-fluomine

The capacity of materials containing Co-fluomine for O_2 binding was evaluated by static volumetric gas uptake measurements at room temperature. The results are reported in Table 6. The dioxygen adsorption isotherm for the material **2-HMS$_4$-[4]** is shown in Fig. 7 and compared to dinitrogen in order to get a blank corresponding to non-selective adsorption of gas on the material. The equilibrium constant for dioxygen binding, K_{O_2}, was calculated using a double adsorption process[46,47] derived by analogy to multiple-site Langmuir-type adsorption model. The dioxygen binding capacity, V_{O_2}, was obtained by subtracting the adsorption of a blank (adsorption of dinitrogen) to the dioxygen isotherm (Fig. 7), to determine

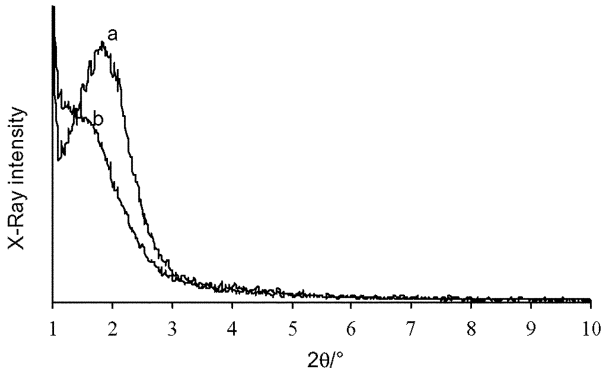

Fig. 6 Powder XRD diffraction patterns for **2-HMS$_{19}$-[4]** (a), **2-HMS$_4$-[4]** (b).

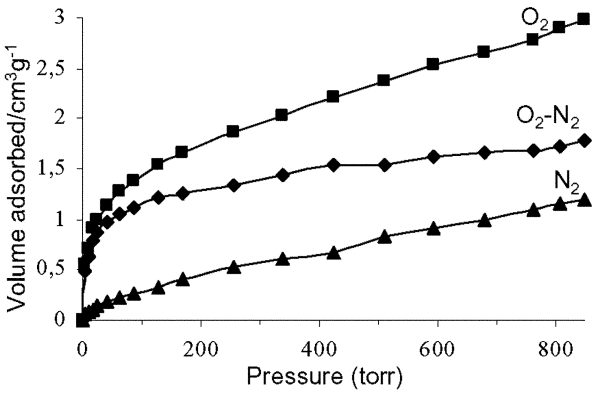

Fig. 7 Nitrogen and oxygen adsorption isotherms of **2-HMS$_4$-[4]**.

Table 6 Thermodynamic data at 293 K for dioxygen adsorption by the hybrid materials incorporating Co-fluomine

Entry	Sample	Treatment before reaction	$V_{O_2}{}^a$ / cm^3 g^{-1}	$V_{N_2}{}^a$ (cm^3 g^{-1})	$(P_{O_2})_{½}{}^{b,c}$ / Torr	% of oxygenation[d]
1	**2-HMS$_4$-[4]**	150 °C, 3 h	2.8	1.1	6.9	17
2	**2-HMS$_6$-[4]**	150 °C, 3 h	1.7	0.5	5.8	14
3	**2-HMS$_6$-Si-[4]**	120 °C, 2 h30	1.4	0.3	1	23
4	**2-HMS$_9$-[4]**	120 °C, 3 h	1.0	0.75	—	3
5	**2-HMS$_9$-Si-[4]**	120 °C, 3 h	0.4	—	—	<< 12
6	**2-SBA-[4]**	120 °C, 2 h	0.7	—	—	<< 12
7	**2-SBA-Si-[4]**	120 °C, 2 h	0.4	—	—	<< 11

[a]Volume adsorbed at 760 Torr. [b]Determined from the Langmuir isotherm (see text). [c]$(P_{O_2})_{½} = 1/K_1$. [d]Assuming a 1 : 1 complex (O_2 : Co).

the increase in dioxygen uptake resulting only from the active dioxygen binding complex.[48,49]

The thermodynamic data presented in Table 6 clearly show that Co-fluomine incorporating materials exhibit a great affinity towards dioxygen with $(P_{O_2})_{½}$ $(=1/K_1)$ varying from 1 to 6.9 Torr, and a total V_{O_2} adsorbed at 760 Torr ranging from 1.4 to 2.8 $cm^3\ g^{-1}$.

It appears that: (i) the adsorption of O_2 increased with the concentration of Co-fluomine (entries 1, 2, 3); (ii) the percentage of sites involved in the oxygenation after silylation of the surface SiOH was slightly superior to that obtained from the corresponding uncapped material (entries 2 and 3) which suggested that the capping of SiOH groups has probably reduced the interactions between SiOH on the surface and the transition metal, interactions that should prevent the dioxygen uptake; (iii) the oxygen uptake for the material **2-SBA-[4]** is inferior to that of the material **2-HMS$_6$-[4]** while the concentration of cobalt is very similar for both materials.

Nature of the bond

Almost all known transition metal dioxygen complexes can be divided into two types[30,45,50–52] according to the characteristics of the dioxygen ligand: the superoxide (O_2^-, type I) and the peroxide (O_2^{2-}, type II) complexes. These complexes are further classified as to whether the dioxygen is bound to one metal atom (type a) or bridges two metal atoms (type b) (Fig. 8). The free Co-fluomine is generally considered to form 1 : 2 (O_2 : Co) adducts (type Ib or IIb shown in Fig. 8).[37] To gain some information concerning the type of complex formed during the exposure of the materials to dioxygen, EPR spectroscopy was used. The EPR spectra of samples **2-HMS$_y$-[4]** (y = 4 and 6) and **2-HMS$_6$-Si-[4]** were recorded at 100 K before and after oxygenation, and the spectra of **2-HMS$_4$-[4]** are presented in Fig. 9. Under strictly anaerobic

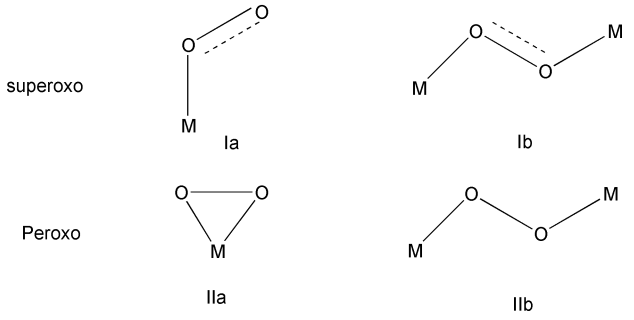

Fig. 8 Types of metal-dioxygen geometries.

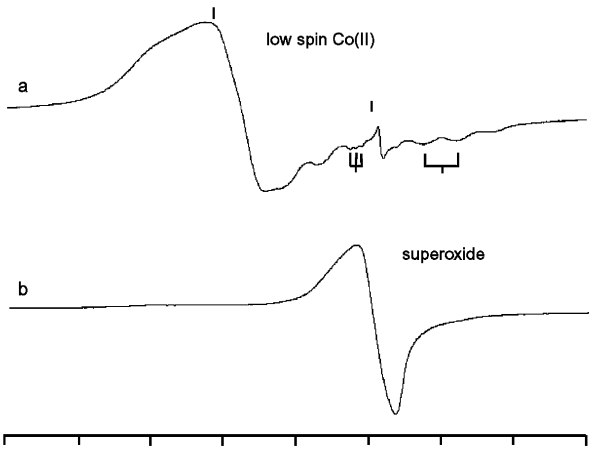

Fig. 9 EPR spectra at 100 K for **2-HMS$_4$-[4]** before (a) and after (b) oxygenation.

conditions, **2-HMS$_4$-[4]** displays a nearly axial anisotropic spectrum with an eight-line hyperfine splitting in the $g_{//}$ region due to ^{59}Co (I = 7/2) nucleus (Fig. 9a). This EPR spectrum is characteristic of a low spin d^7 (S = ½) cobalt(II) complex in a five-coordinate square pyramidal geometry with the unpaired electron localised in the d_{z2} orbital.[50] Moreover, the nitrogen atom of the imidazole axial ligand incorporated in the material gives rise to a three-line superhyperfine coupling (I_N = 1) in the parallel region. The EPR parameters ($g_{//}$ = 2.01, $g_\perp$ = 2.32, $A_{//}^{Co} = 88 \times 10^{-4}\ cm^{-1}$, $A_{//}^{N} = 14.6 \times 10^{-4}\ cm^{-1}$) are typical of a five-coordinate cobalt(II) Schiff base complex,[50] and are similar to the EPR data for porphyrins,[53] peptide derivatives,[54] or cobalamin models.[55]

The EPR spectrum of **2-HMS$_4$-[4]** was dramatically transformed upon exposure to dioxygen (Fig. 9b). The axial anisotropic signal of **2-HMS$_4$-[4]** changes to a more isotropic and symmetrical signal at $g \approx 2$ typical of radical species, attributed to a superoxide entity.[50–52] The $A_{//}^{Co}$ coupling cannot be observed due to a broadening of the lines in the solid state and the decrease in intensity due to a nearly complete delocalisation of the electron density on the dioxygen moiety.

Thus, the experimental data showed that: (i) A superoxide complex was formed when the immobilized Schiff base cobalt(II) complex was exposed to dioxygen; (ii) the dioxygen binding capacity of the materials increased with the proximity of the cobalt centers within the pores. These facts suggested the formation of a μ-superoxo complex of type Ib to the pentacoordinated Co-fluomine incorporated within the meso-structured hybrid materials. This means that the percentage of 1 : 2 (O_2 : Co) adduct is 34% for **2-HMS$_4$-[4]** and 28% for **2-HMS$_6$-[4]**. The weak oxygen uptake for the material **2-SBA-[4]** in comparison to that of the material **2-HMS$_6$-[4]** could be due to a irregular distribution of ligands in the material **2-SBA-[4]**, which is unfavourable to the formation of μ-superoxo complex.

It is worth noting that these results are in the same range as those obtained by immobilisation of the Co-fluomine on aluminosilicate.[37] The absence of residual low spin Co(II) complex after exposure of materials to dioxygen seems to imply that all the active sites were oxygenated, but the experimental O_2 capacities for O_2-binding materials were far from the theoretical capacities for 1 : 2 (O_2 : Co) adducts. As treatment of materials with HMDS did not give rise to a complete silylation of SiOH groups, the inability to bind O_2 for a number of Co(II) centres could be attributed to the coordination of remaining SiOH groups to Co(II) giving rise to diamagnetic Co(III) species (Fig. 10). Another possibility may be the existence of a mixed spin state in the solid, one part of the cobalt complex being in a low spin state, and the other part having a high spin electronic state (S = 3/2) with a low affinity towards dioxygen, as already observed for Schiff base cobalt(II) complexes incorporated in zeolite Y.[56–58]

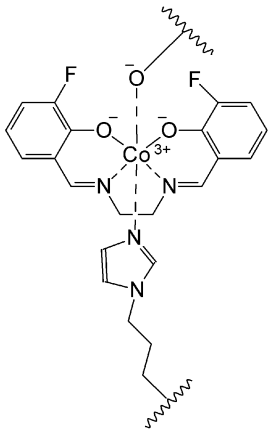

Fig. 10

Conclusion

Immobilisation of Co-salen and Co-fluomine onto ordered mesoporous silica has been achieved through coordination of the cobalt to pyridine or imidazole groups covalently attached to the silica matrix. Two routes have been investigated to obtain mesoporous hybrid materials containing coordinating ligands: post synthesis grafting of the ligand on ordered mesoporous silica or direct synthesis method. The first method gave rise to hexagonally ordered mesoporous hybrid materials. The second afforded mesoporous hybrid materials with a typically disordered wormhole-like pore structure. Interestingly, only this second route allowed the oxygen uptake. As there is probably formation of a μ-superoxo complex, this result can be considered as another probe for the regular distribution of the organic groups by the direct synthesis method in comparison to that obtained by the post-synthesis grafting.

References

1 C. T. Kresge, M. E. Leonowicz, W. J. Roth, J. C. Vartuli and J. S. Beck, *Nature*, 1992, **359**, 710.
2 J. S. Beck, J. C. Vartuli, W. J. Roth, M. E. Leonowicz, C. T. Kresge, K. D. Schmitt, C. T.-W. Chu, D. H. Olson, E. W. Sheppard, J. B. McCullen, J. B. Higgins and J. L. Schlenker, *J. Am. Chem. Soc.*, 1992, **114**, 10834.
3 P. T. Tanev and T. J. Pinnavaia, *Science*, 1995, **267**, 865.
4 E. Prouzet and T. J. Pinnavaia, *Angew. Chem., Int. Ed. Engl.*, 1997, **36**, 516.
5 D. Zhao, Q. Huo, J. Feng, B. F. Chmelka and G. D. Stucky, *J. Am. Chem. Soc.*, 1998, **120**, 6024.
6 C.-J. Liu, S.-G. Li, W.-Q Pang and C.-M. Che, *Chem. Commun.*, 1997, 65.
7 S.-G. Shyu, S.-W. Cheng and D.-L. Tzou, *Chem. Commun.*, 1999, 2337.
8 C. M. Crudden, D. Allen, M. D. Mikoluk and J. Sun, *Chem. Commun.*, 2001, 1154.
9 D. A. Loy and K. J. Shea, *Chem. Rev.*, 1995, **95**, 1431.
10 (*a*) R. J. P. Corriu, *Angew. Chem., Int. Ed.*, 2000, **39**, 1377; (*b*) R. J. P. Corriu, *Eur. J. Inorg. Chem.*, 2001, 1109.
11 L. Mercier and T. J. Pinnavaia, *Adv. Mater.*, 1997, **9**, 500.
12 A. Cauvel, G. Renard and D. Brunel, *J. Org. Chem.*, 1997, **62**, 749.
13 P. M. Price, J. H. Clark and D. J. Macquarrie, *J. Chem. Soc., Dalton Trans.*, 2000, 101.
14 A. M. Liu, K. Hidajat, S. Kawi and D. Y. Zhao, *Chem. Commun.*, 2000, 1145.
15 D. J. Macquarrie, *Chem. Commun.*, 1996, 1961.
16 D. J. Macquarrie, D. B. Jackson, J. E. G. Mdoe and J. H. Clark, *New J. Chem.*, 1999, **23**, 539.
17 R. J. P. Corriu, A. Mehdi and C. Reyé, *C. R. Acad. Sci., Sér. IIc: Chim.*, 1999, 35.
18 C. E. Fowler, S. L. Burkett and S. Mann, *Chem. Commun.*, 1997, 1769.
19 M. H. Lim and A. Stein, *Chem. Mater.*, 1999, **11**, 3285.
20 A. Stein, B. J. Melde and R. C. Schroden, *Adv. Mater.*, 2000, **12**, 1403.
21 L. Mercier and T. J. Pinnavaia, *Chem. Mater.*, 2000, **12**, 188.
22 Y. Mori and T. J. Pinnavaia, *Chem. Mater.*, 2001, **13**, 2173.
23 G. Dubois, R. J. P. Corriu, C. Reyé, S. Brandès, F. Denat and R. Guilard, *Chem. Commun.*, 1999, 2283.
24 G. Dubois, C. Reyé, R. J. P. Corriu, S. Brandès, F. Denat and R. Guilard, *Angew. Chem., Int. Ed.*, 2001, **40**, 1087.
25 L. F. Lindoy, *The Chemistry of Macrocyclic Ligand Complexes*, Cambridge University Press, Cambridge, 1989.
26 P. V. Bernhardt and G. A. Lawrance, *Coord. Chem. Rev.*, 1990, **104**, 297.
27 K. Srinivasan, P. Michaud and K. Kochi, *J. Am. Chem. Soc.*, 1986, **108**, 2309.
28 B. Meunier, *Inorg. Chem.*, 1991, **3**, 347.
29 W. Zhang and E. N. Jacobsen, *J. Org. Chem.*, 1991, **56**, 2296.
30 G. Q. Li and R. Goving, *Ind. Eng. Chem. Res.*, 1994, **33**, 755.
31 M. Calvin and A. E. Martell, *Chemistry of the metal chelate compounds*, Prentice-Hall, New-York, 1952.
32 D. Brunel, N. Belloq, P. Sutra, A. Cauvel, M. Laspéras, P. Moreau, F. D. Renzo, A. Galarneau and F. Fajula, *Coord. Chem. Rev.*, 1998, **178–180**, 1085.
33 A. Choplin and F. Quignard, *Coord. Chem. Rev.*, 1998, **178–180**, 1679.
34 I. C. Chisem, J. Rafeft, M. Tantoh Shieh, J. Chisem, J. H. Clark, R. Jachuck, D. Macquarrie, C. Ramshaw and K. Scott, *Chem. Commun.*, 1998, 1949.
35 P. Sutra and D. Brunel, *Chem. Commun.*, 1996, 2485.
36 X.-G. Zhou, X.-Q. Yu, J.-S. Huang, S. G. Li, L.-S. Li and C.-M. Che, *Chem. Commun.*, 1999, 1789.
37 N. D. Hutson and R. T. Yang, *Ind. Eng. Chem. Res.*, 2000, **39**, 2252.
38 C. Boissière, A. Larbot and E. Prouzet, *Chem. Mater.*, 2000, **12**, 1937.
39 E. Barrett, L. G. Joyner and P. P. Halenda, *J. Am. Chem. Soc.*, 1951, **73**, 373.
40 R. Anwander, C. Palm, J. Stelzer, O. Groeger and G. Engelhart, *Stud. Surf. Sci. Catal.*, 1998, **117**, 135.
41 K. A. Koyano, T. Tatsumi, Y. Tanaka and S. Nakata, *J. Phys. Chem. B*, 1997, **101**, 9436.
42 C.-J. Liu, S.-G. Li, W.-Q. Pang and C.-M. Che, *Chem. Commun.*, 1997, 65.
43 Y. He, J. Yang, H. Li and P. Huang, *Polymer*, 1998, **39**, 3393.
44 K. Kuraoka, Y. Chujo and T. Yazawa., *Chem. Commun.*, 2000, 2477.
45 L. Vaska, *Acc. Chem. Res.*, 1976, **9**, 175.
46 R. S. Drago, C. E. Webster and J. M. McGilvray, *J. Am. Chem. Soc.*, 1998, **120**, 538.
47 C. E. Webster, A. Cottone III and R. S. Drago, *J. Am. Chem. Soc.*, 1999, **121**, 12127.
48 R. J. Taylor, R. S. Drago and J. E. George, *J. Am. Chem. Soc.*, 1989, **111**, 6610.
49 R. J. Taylor, R. S. Drago and J. P. Hage, *Inorg. Chem.*, 1992, **31**, 253.
50 D. R. Jones, D. A. Summerville and F. Basolo, *Chem. Rev.*, 1979, **79**, 139.
51 E. C. Niederhoffer, J. H. Timmons and A. E. Martell, *Chem. Rev.*, 1984, **84**, 137.
52 T. D. Smith and J. R. Pilbrow, *Coord. Chem. Rev.*, 1981, **39**, 295.
53 R. Guilard, S. Brandès, C. Tardieux, A. Tabard, M. L'Her, C. Miry, P. Gouerec, Y. Knop and J. P. Collman, *J. Am. Chem. Soc.*, 1995, **117**, 11721.
54 F. A. Chavez, C. V. Nguyen, M. M. Olmstead and P. K. Mascharak, *Inorg. Chem.*, 1996, **35**, 6282.
55 J. S. Trommel, K. Warncke and L. G. Marzilli, *J. Am. Chem. Soc.*, 2001, **123**, 3358.
56 D. E. De Vos, E. J. P. Feijen, R. A. Schoonheydt and P. A. Jacobs, *J. Am. Chem. Soc.*, 1994, **116**, 4746.
57 D. E. De Vos, F. Thibault-Starzyk and P. A. Jacobs, *Angew. Chem., Int. Ed. Engl.*, 1994, **33**, 431.
58 N. Herron, *Inorg. Chem.*, 1986, **25**, 4714.